Effect of temperature on the corrosion behaviour of low-nickel duplex stainless steel bars in concrete

Matteo Gastaldi *, Luca Bertolini

[a] *Politecnico di Milano, Department of Chemistry, Material and Chemical Engineering, "Giulio Natta", via Mancinelli 7, 20131 Milano, Italy*

Received 9 May 2013
Accepted 7 November 2013
Available online xxxx

1. Introduction

The aggressive nature of tropical marine environments determines great problems of durability for reinforced concrete structures (e.g. bridges and marine piers), due to chloride-induced corrosion of embedded steel bars [1]. The concrete cover itself may not succeed to guarantee long-term corrosion protection of usual carbon steel bars, even if good quality concrete and high cover thickness are considered, and preventative measures are necessary even for a service life of less than 100 years [1–3]. The use of stainless steel bars can provide a durable and maintenance-free solution to corrosion problems in the most critical parts of marine concrete structures, typically the splash, spray or tidal zones [4–6]. To achieve this goal, a correct selection of the grade of stainless steel that can be used on the basis of environmental aggressiveness is needed. As a matter of fact, even though stainless steels offer a corrosion resistance higher than carbon steel, the different grades of stainless steel bars available on the market have different corrosion performances [4,7,8]. To make a proper choice of the stainless steel grade, data on chloride threshold for corrosion initiation are required as a function of the exposure condition (i.e. moisture conditions and temperature of concrete). If the chloride threshold levels for available types of stainless steels are known, the design for durability of reinforced concrete elements can be carried out by selecting a suitable and cost-effective combination of concrete composition, concrete cover thickness and grade of stainless steel, e.g. using deterministic or probabilistic methods [3,9].

Similarly as for conventional carbon steel bars (for which indicative value in the range of 0.4–1% by mass of cement is usually considered under atmospheric exposure [1]), the chloride threshold level of stainless steel bars depends on the temperature and relative humidity of the environment (that influence the temperature and moisture content of the concrete in contact with the steel). This threshold, however, is also remarkably affected by other important factors such as chemical composition, microstructure and surface finish of the steel, steel potential, pH of the concrete pore solution, and presence of voids at the steel/concrete interface [10–14]. Taking also into account that pitting corrosion induced by chlorides is a stochastic phenomenon, the chloride threshold should be defined not by a single value, but by a probability distribution.

The task of defining the chloride threshold is rather difficult. Unfortunately, simple indices, such as the pitting resistance equivalent number (PREN) that is often utilised to rank the corrosion resistance of stainless steels in near-neutral environments, are not reliable in predicting the corrosion performance of steels in alkaline environments [15,16].

Tests in solution are often used to evaluate the corrosion resistance of stainless steel rebars; these tests, however, cannot be used to estimate the chloride threshold in concrete and may even fail in ranking of the corrosion resistance of stainless steels in concrete [16].

To estimate the chloride threshold for pitting corrosion initiation a large number of tests should be carried out in conditions that are representative of the actual steel–concrete interface of real structures [12,13]. Beyond the fact that the actual condition of bars embedded in real structures are rather difficult to reproduce in the laboratory, tests in concrete are in any case time consuming [17].

As a consequence only few data based on tests in concrete are reported in the literature for stainless steel bars embedded in concrete.

* Corresponding author. Tel.: +39 02 2399 3114.
E-mail addresses: matteo.gastaldi@polimi.it (M. Gastaldi), luca.bertolini@polimi.it (L. Bertolini).

Moreover data are generally limited to traditional austenitic stainless steel grades with about 18%Cr and 10% Ni (e.g. grades 1.4307 or 1.4311 according to EN 10088 standard; 304L or 304LN according to ASTM standard) and possibly 2–3%Mo (e.g. 1.4404, 1.4406 or 1.4436; AISI 316L or 316LN), and to exposure to mild temperatures of 20–25 °C [18–24].

Nevertheless stainless steel bars are often used to increase the service life of reinforced concrete structures exposed to marine tropical climates [25] where the aggressiveness of the environment is increased by temperatures that may exceed daily average values of 40 °C with much higher peak values [26]. In these environments, even though concrete has a low thermal conductivity, high temperature may be reached at the depth of the steel bars, leading to a remarkable decrease in the chloride resistance, i.e. on the chloride threshold.

Only few data on other stainless steel grades [27–30] and in hot environments are available [6,31,32]. Particularly, few data are available on different grades of stainless steels with duplex austeno-ferritic microstructure which have been proposed as rebars for concrete [15,27–30]. Initially duplex stainless steel 1.4462, with about 22% Cr, 5%Ni and 3%Mo, was studied and this showed a corrosion resistance in chloride-contaminated concrete even higher than that of austenitic stainless steels [32]. In recent years, the increase in the cost of alloying elements has led to the use of low-nickel and low-molybdenum duplex stainless steels as reinforcing bars, such as 1.4362 (about 23%Cr and 4% Ni) and 1.4162 (about 21%Cr, 1% Ni and 4% Mn). At temperatures of about 20 °C, duplex 1.4362 stainless steel was shown to suffer pitting corrosion in concrete with 3% chloride by cement mass [16]; a lower corrosion resistance in chloride contaminated concrete was observed on 1.4162 [16,28,29]. As far as the effect of high temperature is concerned, results of potentiodynamic polarisation tests at 50 °C in alkaline solutions (pH = 12) with 21 g/L of sodium chloride showed that neither duplex stainless steels (1.4362 and 1.4462) nor traditional austenitic stainless steels (1.4301 and 1.4404) exhibited pitting corrosion initiation [33]. However, no data on the corrosion resistance of these stainless steel grades embedded in concrete exposed to high temperature are available. So the corrosion behaviour in tropical environments of low-nickel duplex stainless steel reinforcing bars still needs to be evaluated.

This paper reports the results of an investigation on the effect of temperature on the corrosion resistance of rebars of low-nickel duplex stainless steels and traditional austenitic stainless steels. Tests in concrete and in solution were carried out in the presence of different concentrations of chloride ions. A detailed description of the results of the tests performed at 20 °C is reported in reference [16], in which different test procedures to estimate the critical chloride content for corrosion initiation in solution and in concrete are compared. This paper describes results of tests at temperatures in the range 20–60 °C and focuses on the effect of increasing temperature on the chloride threshold.

2. Experimental procedure

Tests were carried out on commercial rebars of two grades of low-nickel duplex stainless steels (1.4162 and 1.4362) and, for comparison, two grades of austenitic stainless steels (1.4311 and 1.4406). Table 1 shows the chemical composition and mechanical properties of the steel bars. The surface of the bars was subjected to ordinary commercial pickling; in order to remove all the potential contamination on the steel surface, the bars received in the lab were further pickled and degreased with acetone. Microstructure of the stainless steels were analysed and results are reported in Ref. [16].

Table 2
Mix proportions of concrete.

Water/cement ratio (w/c)	Cement[a] (kg/m^3)	Water (kg/m^3)	Aggregate[b] (kg/m^3)	Chloride (%)[c]
0.65	300	195	1830	0, 3, 5 and 8
0.5	350	175	1840	5 and 8

[a] Type: CEM II/B-L 32.5R (EN 197-1 standard).
[b] Crushed limestone aggregate, maximum size 9 mm.
[c] By mass of cement, added to the mixing water as calcium chloride.

2.1. Tests in concrete

Bars were embedded in concrete with water/cement ratio of 0.5 and 0.65 and limestone–portland cement (CEM II/B-L 32.5R; EN 197-1 standard) was utilised (Table 2). Concrete with different chloride contents (0, 3%, 5% and 8% by mass of cement added as $CaCl_2$) was cast with a *w/c* ratio 0.65 (two replicate specimens were prepared for each chloride contamination). In order to study the possible role of the water/cement ratio on the chloride threshold concrete with *w/c* ratio 0.5 was also cast with 5% and 8% of mixed-in chloride by mass of cement. Each specimen embedded a bar of each grade of stainless steel. The bars had a concrete cover thickness of 10 mm at the side of casting.

A mixed-metal oxide activated titanium (MMO) wire was fixed near each bar, to be used as reference electrode for measurements of corrosion potential, and a mesh of MMO was embedded in each specimen, to be used as a counter-electrode for electrochemical tests. Concrete specimens without mixed-in chloride were subjected to chloride penetration in order to promote chloride penetration through the concrete cover, reproducing condition of ingress of chloride similar to those expected in real structures. Chloride penetration was carried out by means of ponding with a solution of 35 g/L of sodium chloride for about five months; during this period the chloride content in the concrete at depth of 10–20 mm, representative of the position of the steel bars, reached a value of about 2.5% by cement mass, as described in Ref. [16]. Specimens with both mixed-in and penetrated chlorides were placed in a climatic chamber at 20 °C and 90% R.H. for at least three weeks. Afterwards the temperature was increased to 40 °C, 50 °C and 60 °C and then it was returned to 20 °C. Each step of temperature was maintained for at least one week. Corrosion potential and corrosion current density of the bars were monitored. Corrosion potential was measured versus activated titanium electrodes embedded close to the surface of each bar as well as versus an external calomel reference electrode. Corrosion current density was estimated by means of the polarisation resistance technique. The polarisation resistance was measured by imposing potential steps of ±10 mV versus the free corrosion potential and measuring the current density circulating after 30 s of polarisation. The corrosion current density was calculated as: $i_{corr} = R_p/B$, and a value of 26 mV was considered for the parameter *B* [34].

Table 1
Chemical composition and mechanical properties of stainless steel bars.

Designation		Alloy elements (% by mass)										Y.S	U.S.
EN 10088-1	ASTM/UNS	C	Si	Cr	Ni	Mo	Mn	N	P	S	Cu	(MPa)	(MPa)
1.4406	361LN	0.017	0.58	17.53	11.26	2.56	1.11	0.14	0.033	0.001	–	558	783
1.4311	304LN	0.017	0.42	18.71	8.58	–	1.22	0.16	0.028	0.001	–	790	882
1.4362	S32304	0.024	0.49	23.13	4.49	0.25	1.46	0.137	0.025	0.001	0.14	633	774
1.4162	S32101	0.048	0.8	22.07	1.18	0.02	4.14	0.212	0.024	0.001	–	513	761

At the end of the temperature cycles, potentiostatic polarisation tests at 200 mV vs SCE were performed at 20 °C. The anodic polarisation was maintained for 24 h or until a polarisation current density higher than 100 mA/m^2 was measured.

Finally the concrete specimens were demolished and the surface of the stainless steel bars was analysed. The corroded area was estimated by means of image analysis.

2.2. Tests in solution

Tests in solution were also carried out to study the anodic behaviour of the stainless steel bars. Specimens with 20 mm of the ribbed surface exposed were immersed in saturated calcium hydroxide solutions (pH = 12.6) with different chloride concentrations (added as sodium chloride). Tests were carried out at 20 °C and 40 °C; the temperature of the solution was controlled with a vertex thermometer and a sealed cell with a water-cooled spherical condenser. The specimens were initially immersed in the saturated calcium hydroxide solution free of chloride for at least 24 h, and then chlorides were added 24 h before starting polarisation tests.

Potentiodynamic polarisation tests were carried out in solutions with 1% and 3% of chloride by mass, by imposing a potential scanning of 20 mV/min. Potentiostatic polarisation tests were also carried out by imposing a potential of 200 mV SCE to the steel and adding 0.5% of chlorides to the solution at intervals of 48 h. Tests were interrupted when the polarisation current exceeded 5 A/m^2 (due to corrosion initiation) or a concentration of 7% of chloride by mass was reached.

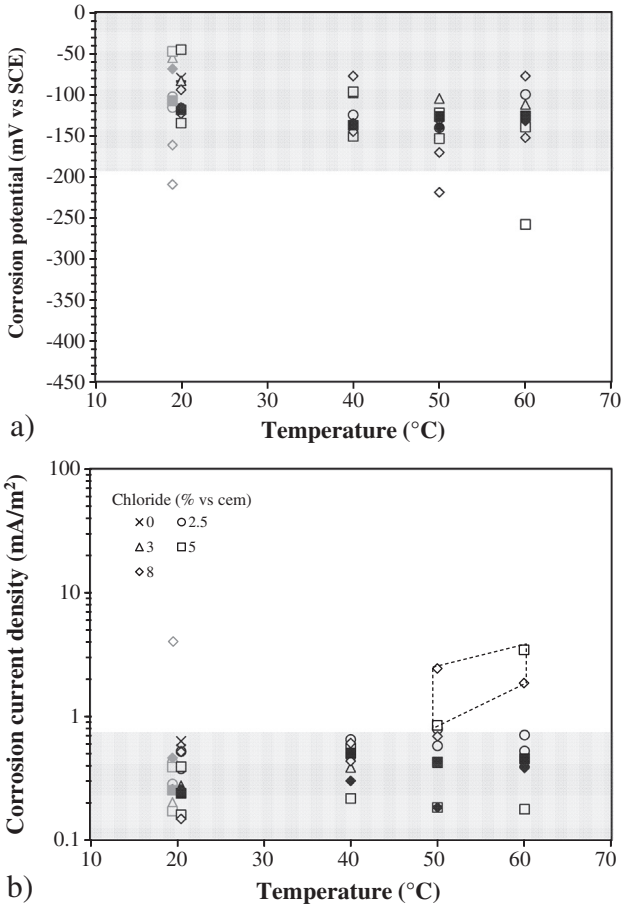

Fig. 1. Effect of temperature on corrosion potential (*a*) and corrosion current density (*b*) of 1.4311 stainless steel bars in concrete specimens with different chloride contents, exposed 90% R.H. (filled symbols = *w/c* of 0.5; unfilled symbols = *w/c* of 0.65; grey symbols = temperature returned at 20 °C after higher temperature cycles).

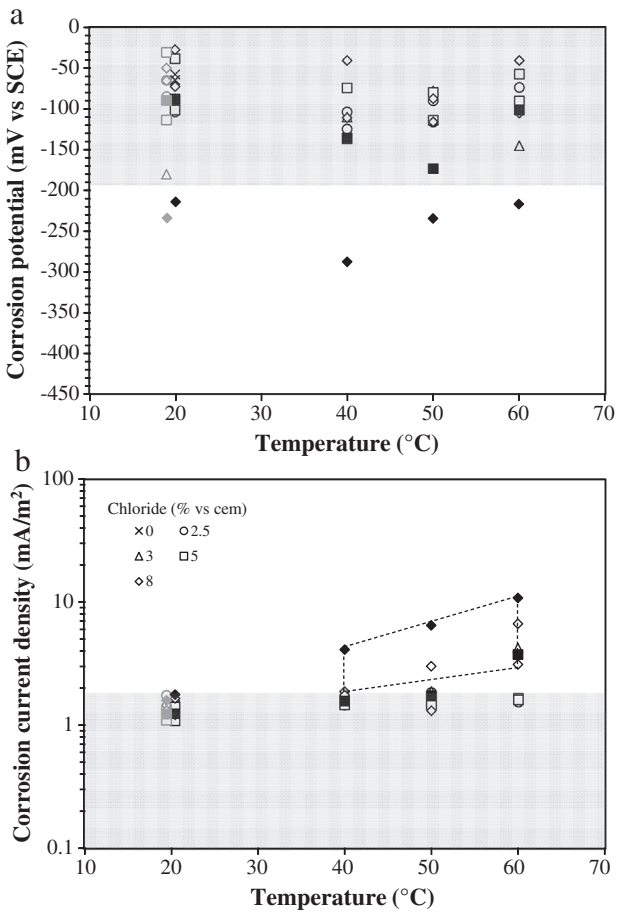

Fig. 2. Effect of temperature on corrosion potential (*a*) and corrosion current density (*b*) of 1.4406 stainless steel bars in concrete specimens with different chloride contents, exposed 90% R.H. (filled symbols = w/c of 0.5; unfilled symbols = w/c of 0.65; grey symbols = temperature returned at 20 °C after higher temperature cycles).

At the end of each test in solution, the exposed surface of the specimens was observed, in order to evaluate if pitting or crevice corrosion had occurred. If crevice corrosion took place the result was not considered and the test was repeated.

3. Results

3.1. Tests in concrete

Figs. 1–4 show the corrosion current density, measured by linear polarisation resistance measurements, and the corrosion potential of the stainless steel bars embedded in concrete specimens with different chloride contents as a function of temperature (average of values measured during one week of exposure at each temperature step are reported). Results of tests carried out when the temperature was returned to 20 °C after exposure at 60 °C are also shown by grey symbols (data measured at 20 °C have been plotted in Figs. 1–4 at a temperature slightly different than 20 °C to avoid overlapping between the two steps at this temperature). As far as specimens without mixed-in chlorides are concerned, both values measured at 20 °C in the first period of ponding, when steel was passive in contact with chloride-free concrete (marked as 0% Cl^- in the figure), and values at the end of the ponding, when a chloride content of about 2.5% by mass of cement was measured at the steel surface [16], are shown.

Shadowed areas in Figs. 1–4 delimit the range of values of corrosion current density and corrosion potential which were measured on passive steels in chloride-free concrete at 20 °C. These areas can be

assumed as representative of the fields were steels are passive, whilst results that lay outside this area may be considered representative of pitting corrosion initiation. As described in details in Ref. [16] the corrosion potential of passive stainless steels ranged between −50 and −180 mV vs SCE regardless of the type of steel and, thus, the passive area in the graphs showing corrosion potential (parts *a* of Figs. 1–4) is defined by values higher than −180 mV vs SCE. Conversely, the corrosion current density of passive steel changed for different steels and, thus, the passive areas in the graphs of corrosion current density (parts *b* of Figs. 1–4) are defined by the upper limit of the corrosion current density measured at 20 °C in chloride-free concrete on each grade of stainless steel [16].

During exposure at 20 °C, austenitic stainless steels showed values of corrosion current density and potential that remained within the shadowed area, even in the concrete specimen with chloride content up to 8% by mass of cement (Figs. 1 and 2). Pitting corrosion initiated at higher temperatures, where results outside the shadowed areas can be observed in Figs. 1 and 2 (for clarity, corrosion current density of values outside the shadowed area was delimited by dashed lines). In concrete with 8% of chloride an increase in corrosion current density and a decrease in corrosion potential were observed starting at 50 °C on 1.4311 (Fig. 1) and at 40 °C on 1.4406 (Fig. 2). Values of corrosion current density of 2.5 mA/m^2 and 4 mA/m^2 were measured. The corrosion current density further increased when the temperature rose to 60 °C. In concrete specimens with lower chloride content, corrosion current densities outside the shadowed area were measured in some

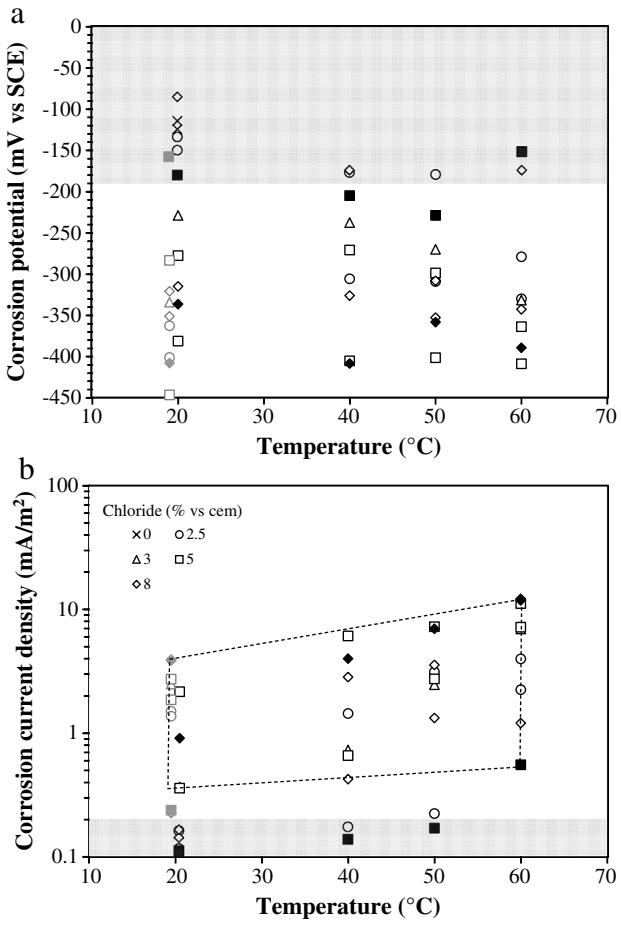

Fig. 3. Effect of temperature on corrosion potential (*a*) and corrosion current density (*b*) of 1.4162 stainless steel bars in concrete specimens with different chloride contents, exposed 90% R.H. (filled symbols = w/c of 0.5; unfilled symbols = w/c of 0.65; grey symbols = temperature returned at 20 °C after higher temperature cycles).

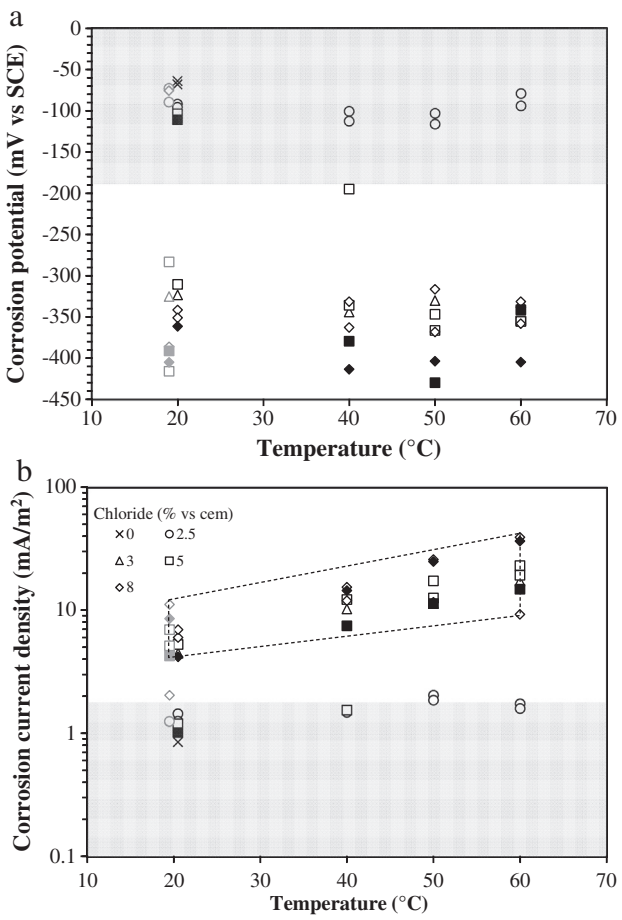

Fig. 4. Effect of temperature on corrosion potential (*a*) and corrosion current density (*b*) of 1.4362 stainless steel bars in concrete specimens with different chloride contents, exposed 90% R.H. (filled symbols = w/c of 0.5; unfilled symbols = w/c of 0.65; grey symbols = temperature returned at 20 °C after higher temperature cycles).

of the specimens only at 60 °C on 1.4311 steel in concrete with 5% of chloride and 1.4406 steel in concrete with 3% of chloride. When the temperature was returned to 20 °C, the corrosion current density of the steels returned to values similar to that of passive steel regardless of the chloride content. Only one bar of 1.4311 steel in concrete with 8% of chloride maintained higher values of corrosion current density, Fig. 1; in one specimen with 8% of chloride the bar of 1.4406 steel showed a corrosion potential lower than −200 mV vs SCE returning to 20 °C, although the corrosion current density in this case was in the shadowed passive field (Fig. 2).

Figs. 3 and 4 show the effect of temperature on the corrosion current density and corrosion potential of duplex stainless steels 1.4162 and 1.4362. Values outside the shadowed area, showing corrosion initiation, can be observed even at 20 °C in concrete with 3% of chloride. The corrosion current density increased as the temperature increased.

In the duplex 1.4162 steel (Fig. 3) the onset of corrosion was detected at 40 °C even in the concrete specimen subjected to ponding, i.e. with 2.5% by mass of chloride at the steel surface; corrosion current density one order of magnitude higher than that measured in passive conditions and corrosion potential lower than −300 mV vs SCE were measured. The increase in temperature caused the corrosion initiation on all the bars of this steel; corrosion current densities higher than 10 mA/m^2 were measured during exposure at 60 °C. When temperature returned to 20 °C, corrosion current densities remained high.

On 1.4362 steel the exposure at higher temperature caused an increase in corrosion current density on the bars already depassivated at 20 °C (Fig. 4) and further induced corrosion initiation in all the other

Table 3
Results of potentiostatic tests and visual observation of bars: Cl^- = mixed-in chloride content (% by mass of cement), I_{corr}, E_{corr} = corrosion current density and corrosion potential measured at 20 °C after temperature cycles; I_{pol} = anodic current density measured after 24 h of potentiostatic polarisation at 200 mV vs SCE; *Attack* = description of the corrosion attack observed at the end of tests; W_{max} = maximum size of the corrosion attack; A = percentage of corroded area.

Steel grade	Concrete		I_{corr} (mA/m^2)	E_{corr} (mV/SCE)	I_{pol} (mA/m^2)	*Attack*	W_{max} (mm)	A (%)
	Cl^-	w/c						
1.4311	2.5[a]	0.65	0.28	−103	168	Shallow	1–2	0.01
		0.65	0.43	−116	13.6	Shallow	10	1.30
	3	0.65	0.20	−56	0.50	–	–	–
	5	0.65	0.39	−48	0.80	Deep	5	0.15
		0.65	0.17	−108	0.30	Shallow	1	0.01
		0.5	0.25	−108	0.40	–	–	–
	8	0.65	4.02	−210	1493	Shallow/deep	10	22.25
		0.65	0.26	−162	0.30	–	–	–
		0.5	0.46	−69	411	Shallow	10	0.35
1.4406	2.5[a]	0.65	1.76	−65	154	Shallow	1	0.14
		0.65	1.38	−85	1.69	–	–	–
	3	0.65	1.56	−180	0.03	Deep	40	0.70
	5	0.65	1.21	−31	1.00	–	–	–
		0.65	1.10	−114	0.80	Shallow	2	0.14
		0.5	1.24	−90	0.90	Deep	10	0.75
	8	0.65	1.46	−50	2.99	Deep	7	0.15
		0.65	1.32	−66	1.99	Deep	10	0.90
		0.5	1.60	−234	192	Deep	40	1.50
1.4162	2.5[a]	0.65	1.50	−363	360	Deep	10	1.40
		0.65	1.37	−401	27	Shallow/deep	10	1.19
	3	0.65	2.49	−334	834	Deep	20	8.65
	5	0.65	1.86	−284	–	Deep	30–40	4.95
		0.65	2.73	−447	244	Deep	40	5.58
		0.5	0.24	−158	–	Shallow	1	0.02
	8	0.65	3.87	−321	–	Deep	30	5.93
		0.65	0.23	−351	84	Shallow	6	0.87
		0.5	3.93	−408	–	Deep	40	7.40
1.4362	2.5[a]	0.65	1.26	−73	323	Shallow	2	0.80
		0.65	1.26	−90	1.99	(Stains)	–	–
	3	0.65	5.21	−325	91	Deep	50	6.95
	5	0.65	6.93	−283	–	Deep	10–20	2.75
		0.65	5.13	−416	91	Deep	45	5.75
		0.5	4.24	−391	–	Deep	40	5.70
	8	0.65	2.03	−76	–	Deep	30	2.95
		0.65	11.12	−386	170	Deep	30	3.50
		0.5	8.51	−405	–	Deep	45	5.35

[a] Chloride content estimated at the depth of bars at the end of ponding tests.

specimens with 3–8% chlorides added in the mix. Corrosion current densities of 9–40 mA/m^2 were measured during exposure at 60 °C. Only the bars in the specimens with 2.5% chloride by mass of cement did not show results outside the passive area during the high temperature tests.

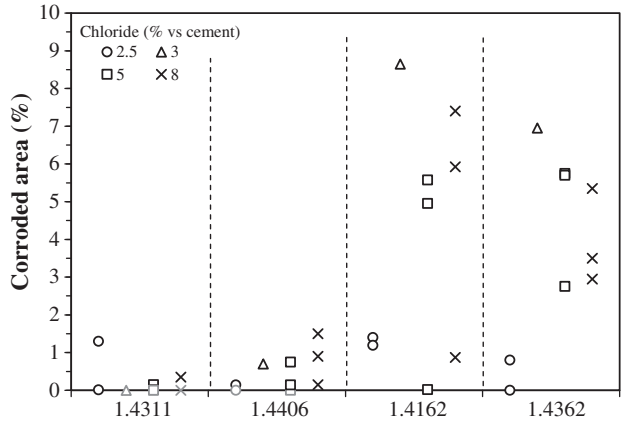

Fig. 5. Percentage of corroded area estimated (by means of an image analysis software) at the end of the tests on the surface of the different grades of stainless steel bars in concrete specimens with different chloride contents (grey symbols = no macroscopical corrosion observed).

No significant difference in corrosion behaviour of the stainless steel bars was observed in specimens with different w/c ratio.

To further investigate the corrosion conditions of stainless steel bars at the end of the temperature cycles, results of potentiostatic polarisation tests can be considered. Table 3 reports the anodic current density (I_{pol}) measured after 24-hours of potentiostatic polarisation at 200 mV vs SCE; the corrosion current density (I_{corr}) and corrosion potential (E_{corr}) measured at 20 °C just before the application of the anodic polarisation (i.e. after the high temperature cycle) are also shown for comparison.

High values of current density were measured during the anodic polarisation in the rebars of 1.4311 in two of the three concrete specimens with 8% of chloride by cement mass (Table 3), showing the pitting corrosion was initiated on these bars. In concrete with 5% of chloride, where corrosion initiation was detected during exposure at 60 °C (Fig. 1), values of current density lower than 1 mA/m^2 were measured during the potentiostatic anodic polarisation tests. The potentiostatic polarisation induced on 1.4311 steel current density values of 13 and 170 mA/m^2 in the concrete specimens subjected to ponding with 2.5% of chloride by cement mass at the steel surface.

In 1.4406 steel (Table 3) high values of current density (>100 mA/m^2) during the potentiostatic tests were measured only in one specimen in concrete with 8% of chloride, that has already showed corrosion initiation at 40 °C (Fig. 2), and on one bar in concrete specimen subjected to ponding. On the other bars, even those that showed corrosion initiation at high temperature, the current density decreased during

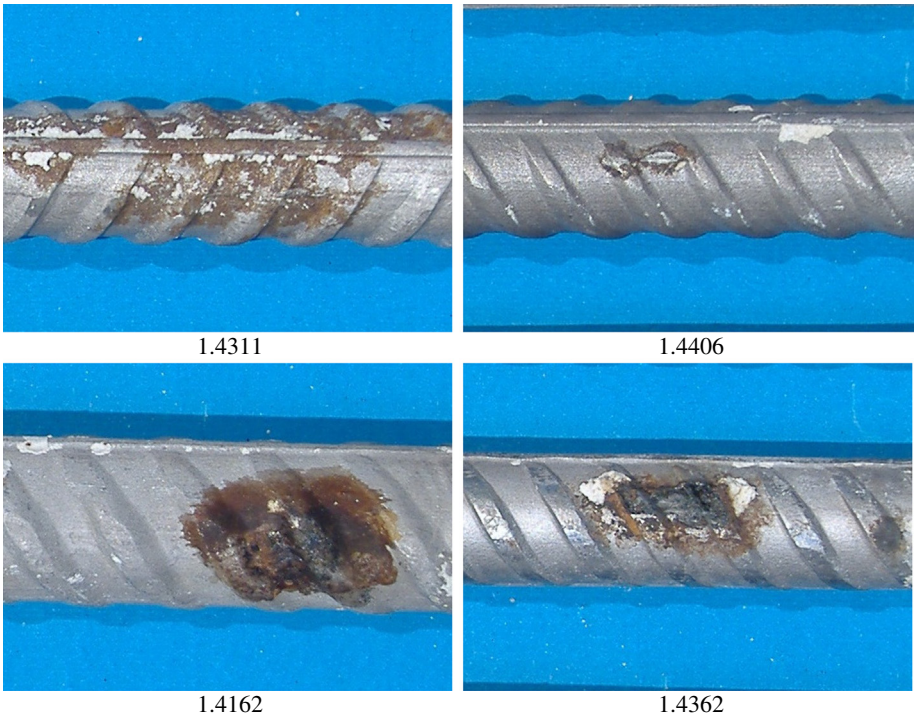

Fig. 6. Examples of corrosion attacks observed after concrete demolition on the surface of the rebars embedded in concrete with 8% of chloride by cement mass and *w/c* ratio of 0.65.

Table 4
Summary of results of tests in concrete; cells of the table are coloured in grey when corrosion evidence was observed (pot. = potentiostatic polarisation at 200 mV vs SCE; obs. = visual observation).

Steel	*T* (°C)	Chloride (% by cement) 2.5*	3	5	8
1.4311	20				
	40				
	50				
	60				
	20				
	Pot.				
	Obs.				

Steel	*T* (°C)	Chloride (% by cement) 2.5*	3	5	8
1.4406	20				
	40				
	50				
	60				
	20				
	Pot.				
	Obs.				

Steel	*T* (°C)	Chloride (% by cement) 2.5*	3	5	8
1.4162	20				
	40				
	50				
	60				
	20				
	Pot.				
	Obs.				

Steel	*T* (°C)	Chloride (% by cement) 2.5*	3	5	8
1.4362	20				
	40				
	50				
	60				
	20				
	Pot.				
	Obs.				

* Specimens subjected to ponding, chloride content estimated at the depth of the bars at the end of ponding tests.

the 24 h of the potentiostatic tests and values lower than 2–3 mA/m^2 were measured at the end of the tests.

Potentiostatic anodic polarisation tests carried out on 1.4162 and 1.4362 steels were carried out only on bars that had not shown corrosion initiation during the previous tests, detected by high corrosion current density and low corrosion potential (Figs. 3 and 4), and on at least one bar for any chloride content. In all the tested specimens current density ranging from 27 to more than 800 mA/m^2 was measured (Table 3).

Table 3 and Fig. 5 summarize the results of the visual observation of the surface of the bars at the end of the tests. Bars were observed after gentle removal of the adherent concrete, in order to have an overall evaluation of the extension of the corroded area. Since bars were not pickled, the actual extension of pitting attack is expected to be lower. Fig. 6 reports examples of the corrosion attacks observed on the surface of the stainless steel bars in concrete with 8% of chloride by mass of cement and w/c ratio of 0.65. Few and small corrosion attacks were observed on the surface of austenitic stainless steels (Table 3), for which the corroded area was less than 2% of the surface of the bars (Fig. 5). On 1.4406 steel the attack often initiated in small defects (scratches) present on the surface (Fig. 6). Only on a bar of 1.4311 steel in concrete with 8% of chloride by cement mass, a corroded surface higher than 20% was observed (this result is not shown in Fig. 5), although the attacks were shallow (Fig. 6). Visual observation confirmed the presence of severe and deep pitting attacks on the duplex stainless steels (Table 3 and Fig. 6). The corroded area ranged between 1 and 9% in most of the specimens; the extension was less than 1.5% only in the specimens subjected to ponding (2.5% Cl^- in Fig. 5).

3.2. Tests in solution

Fig. 7shows the results of potentiodynamic anodic polarisation tests carried out in saturated calcium hydroxide solutions at 20 and 40 °C. Values of pitting potential (identified with letter *p*) or the upper limit of the passive range due to oxygen evolution for specimens that did not initiate corrosion (pitting corrosion initiation above the upper limit of the passive range is also indicated; at these values of the potential, i.e. about 500–600 mV vs SCE, the reaction of oxygen evolution takes place and probably pitting corrosion is further promoted by acidification) are plotted as a function of temperature and chloride concentration. At 40 °C corrosion initiated on duplex 1.4162 and austenitic 1.4311 stainless steels in the solution with 1% of chloride by mass, although the pitting potential was higher than 250 mV vs SCE. In the solution with 3% chlorides, corrosion initiated on all the stainless steels at pitting potentials between 200 and 500 mV vs SCE. Even 1.4406 steel, on which at 20 °C no corrosion was observed even in solution with 8% of chloride (see Ref. [16] for details of tests at 20 °C), showed a pitting potential of about 330 mV vs SCE in one of the specimen in the solution with 3% of chloride by mass, whilst corrosion did not initiate on the other specimen. Duplex 1.4362 steel showed pitting potential values higher than those of 1.4311 steel. Duplex 1.4162 stainless steel showed the lowest pitting potentials, reaching values as low as 200 mV vs SCE in the solution with 3% of chloride at 40 °C.

Results of potentiostatic polarisation tests at 200 mV vs SCE in which chloride ions were dissolved progressively in the solution (0.5% by mass was added at 48-hour intervals) are shown in Fig. 8. The levels of chloride concentration that led to the initiation of corrosion, which was detected by an increase of the polarisation current density to values higher than 0.5 mA/m^2, are reported by black symbols (whilst white symbols show the steps at which corrosion did not initiate).

Grade 1.4406 stainless steel did not suffer pitting corrosion even at chloride concentration of 10% or 7% by mass respectively at 20 °C and 40 °C. The other steels showed corrosion initiation at 20 °C when chloride concentrations of 6.5–10%, 7.5–8% and 3.5–6% were reached respectively by grades 1.4311, 1.4362 and 1.4162. The increase in temperature to 40 °C led to a considerable decrease in the critical chloride concentration to values of respectively 2–3%, 1–7% and 2% for the three grades of stainless steel (a great variability was observed between the two replicate specimens of 1.4362 steel).

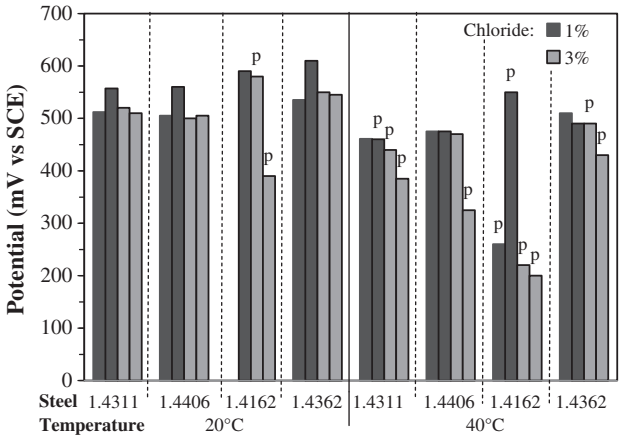

Fig. 7. Pitting potential (p) and upper limit of the passive range (for specimens that did not initiate corrosion) obtained by potentiodynamic tests in saturated calcium hydroxide solution at 20 °C and 40 °C with different chloride concentrations.

4. Discussion

Results presented in the previous section allow an evaluation of the resistance to chloride-induced corrosion of recently proposed low-nickel stainless steels in comparison to that of traditional austenitic stainless steels embedded in concrete exposed to temperatures typical of tropical climates. The role of temperature was investigated by means of tests in concrete and in solution. Tests in concrete were performed with specimens with chloride mixed-in and penetrated. Chlorides were mixed-in in order to reach high values of chloride (up to 8% by mass) at steel surface, expected to initiate corrosion on stainless steel bars, difficult to achieve through ponding. Although this different procedure of chloride-contamination may have some consequences on the concrete (e.g. in the microstructure or in chloride binding [1]), tests carried out at 20 °C showed a good agreement between results obtained with mixed-in and penetrated chlorides.

By comparing of the corrosion behaviour of bars embedded in the concrete specimens with different chloride contamination, an approximate estimation of the range in which the chloride threshold lays can be made. Table 4 summarises the results of the tests in concrete showing the conditions where corrosion evidence was found. Each column

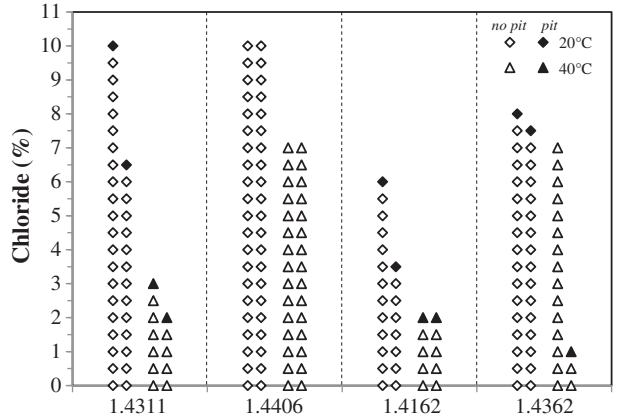

Fig. 8. Chloride content for pitting corrosion initiation (filled symbols) in potentiostatic polarisation tests at 200 mV vs SCE in saturated calcium hydroxide solution at 20 °C and 40 °C (duplicate specimens).

describes the sequence of events to which a bar of a specific steel grade, which was embedded in concrete with a given chloride content, was subjected, i.e. the exposure cycles at 20, 40, 50, 60 and again 20 °C followed by potentiostatic polarisation at +200 mV SCE (at 20 °C) and then by visual observation. Cells of the table are coloured in grey when corrosion evidence was observed. For tests of free corrosion exposure at different temperatures, this condition was associated with the presence of both corrosion current density and corrosion potential values outside the shadowed regions of Figs. 1–4. For the potentiostatic polarisation tests, corrosion detection was associated with the presence of a polarisation current density higher than 100 mA/m^2 at least on one of the replicate bars. Finally for the visual observation, corrosion was associated with the presence of at least a pit on one of the replicate bars (even a tiny and shallow pit). Results obtained on concrete with different *w*/*c* ratio were considered collectively, since no significant effect of *w*/*c* ratio could be observed with the tests described in this work.

Table 4 shows that exposure at high temperature (from 40 to 60 °C) and 90% R.H. caused a decrease in the corrosion resistance of stainless steels. Traditional austenitic stainless steels, showed higher corrosion resistance compared to low-nickel duplex stainless steels. Austenitic stainless steel grade 1.4311 showed corrosion initiation only in the bars embedded in concrete with 5 and 8% of mixed-in chlorides by mass of cement. Corrosion initiation, however, was detected only at 50 °C in concrete with 8%Cl^- and 60 °C in concrete with 5%Cl^-. In the latter, when temperature returned at 20 °C corrosion current density similar to values typical of passive condition was determined and even during subsequent potentiostatic tests at +200 mV corrosion was not detected. This suggests that at 20 °C corrosion attack does not propagate, probably due to repassivation of the corrosion attacks previously initiated during exposure at 60 °C [35,36].

In the specimen with penetrated chlorides (2.5% chloride in Table 4), no corrosion was detected during high temperature cycles. However, corrosion was detected during the potentiostatic tests and it was confirmed by the observation of shallow pits on the surface of the bars at the end of the tests. The initiation of corrosion during the potentiostatic step suggests that, although corrosion did not occur at the free corrosion potential, its initiation was in an incipient state, since a slight increase in potential promoted it.

Austenitic steel 1.4406 showed a slightly worse behaviour compared to 1.4311. In fact, corrosion initiated also in concrete with 3% Cl^- at 60 °C, and in concrete with 8%Cl^- it was detected even at 40 °C (Table 4); also for this type of stainless steel no propagation of the corrosion attacks [35–38] was measured when temperature returned to 20 °C. Conversely, in tests in solution 1.4406 steel showed the best corrosion behaviour. No corrosion was detected during potentiostatic polarisation tests in alkaline solution at 20 °C and 40 °C up to 10% and to 7% of chloride by mass respectively (Fig. 8). Similarly, in potentiodynamic polarisation tests at 40 °C corrosion took place only in the presence of 3% of chloride and at potential values higher than 300 mV vs SCE (Fig. 7).

The lower corrosion resistance observed for this steel embedded in concrete, compared to the less alloyed 1.4311 steel, can be associated to the presence of mechanical defects (scratches generated during manufacturing, Fig. 6) which promoted pitting corrosion initiation, overwhelming the effect of the presence of molybdenum (element that anyway may have a minor beneficial effect on the corrosion resistance of stainless steels in alkaline environments, as observed in [15]). A size effect may explain differences between tests in solution and in concrete. Small specimens (length of 15–20 mm) were used for tests in solution, which were selected to avoid the presence of surface defects visible to the naked eye; conversely, in concrete tests the length of the bars was of about 150 mm, thus the probability to include defects on the steel surface increased.

In both the low-nickel duplex stainless steels corrosion took place in concrete with 3% of mixed-in chloride by mass of cement even during exposure at 20 °C (Table 4). Corrosion current density further increased at higher temperature (Figs. 3 and 4) leading to penetrating corrosion attacks (Table 3) on a large portion of the steel surface (Fig. 5).

No corrosion was detected in the specimens with penetrated chloride on the bars of 1.4362 grade steel. Conversely, on 1.4162 steel, with lower nickel content (1%) and about 4% manganese, corrosion was detected even in the specimens with penetrating chloride beginning from the step at 40 °C (Table 4). This confirms the lower corrosion resistance for this steel, which was also observed with the tests in solution (Figs. 7 and 8). The low corrosion resistance of this steel should be attributed to the low nickel and high manganese content. The negative effect of manganese on the pitting corrosion resistance of stainless steels was reported by the other authors [38–40]. Also the microstructure may have a negative effect on the corrosion resistance, in fact a high percentage of ferritic phase (47%) was observed (for 1.4362 steel the ferritic phase was of 37%) [16].

Although any estimation of the chloride threshold for corrosion initiation of steel bars in concrete is quite difficult and should be supported by a large number of experimental results which allow a statistical analysis, some general features can be delineated. It should be observed that the actual corrosion behaviour of stainless steel bars also strongly depends on the surface condition (being reduced, for instance, by oxide layers not properly removed after the production). Therefore, the following numbers can only be considered as indicative values for a comparison of bars with composition and microstructure similar to that of the bars tested in this work and with the surface cleaned by pickling.

For the austenitic stainless steels 1.4311 and 1.4406 a decrease of the chloride threshold from values higher than 8% by cement mass in mild environment (20 °C), to 5–8% at 40–50 °C and to 2.5–5% at extreme temperature of 60 °C can be estimated. For the low-nickel duplex stainless steels 1.4162 and 1.4362 lower values of 2.5–3% by cement mass could be assumed even in temperate climates (i.e. considering results at 20 °C).

5. Conclusions

In hot and moist environments contaminated by chloride ions, traditional austenitic stainless steels 1.4311 and 1.4406 showed a higher corrosion resistance compared to low-nickel duplex stainless steel 1.4362 and 1.4162. On the latter steels, pitting corrosion took place in concrete with 3% of mixed-in chloride by mass of cement even during exposure at 20 °C. The increase of temperature to 40 °C caused corrosion initiation on 1.4162 stainless steel even in concrete with 2.5% Cl^-. By increasing the temperature up to 60 °C a further increase in corrosion rate was detected, leading to penetrating corrosion attacks on a large part of the steel surface.

Austenitic stainless steels showed no corrosion initiation at 20 °C in concrete with up to 8% of mixed-in chloride by cement mass, whilst corrosion took place in concrete with 8% Cl^- at 40–50 °C and 3–5% Cl^- at 60 °C. Moreover negligible corrosion rates were measured when temperature was restored at 20 °C, suggesting no propagation of the corrosion attacks in all the bars in concrete contaminated with less than 8% of chloride.

The higher corrosion resistance of the traditional austenitic stainless steels was confirmed also by tests in alkaline solutions contaminated by chloride. Duplex 1.4162 stainless steel exhibited the lowest corrosion resistance; at 40 °C pitting potentials reached values as low as 200 mV vs SCE in the solution with 3% of chloride by mass and pitting corrosion took place with 2% of chloride during potentiostatic polarisation tests (at 200 mV vs SCE). Austenitic 1.4406 stainless steel showed the best corrosion behaviour; no corrosion was detected during potentiostatic polarisation tests at 20 °C and 40 °C up to 10% and to 7% of chloride by mass and only at 40 °C a pitting potential value higher than 300 mV vs SCE was observed.

Acknowledgements

The authors are grateful to Acciaierie Valbruna S.p.A. for providing the bars and financing this research.

References

[1] L. Bertolini, B. Elsener, P. Pedeferri, E. Redaelli, R.B. Polder, Corrosion of Steel in Concrete: Prevention, Diagnosis, Repair, 2nd edition Wiley-VCH, Weinheim, 2013.
[2] P.B. Bamforth, G.F. Chapmann-Andrews, Long term performance of RC elements under UK coastal exposure condition, Proc. of Int. Conf. "Corrosion and Corrosion Protection of Steel in Concrete", Sheffield, 24–28 July, 1994, pp. 139–156.
[3] L. Bertolini, Steel corrosion and service life of reinforced concrete structures, Struct. Infrastruct. Eng. 4 (2008) 123–137.
[4] The Concrete Society, Guidance on the use of stainless steel reinforcement, Technical Report No. 51, 1998.
[5] In: U. Nürnberger (Ed.), Stainless Steel in Concrete, European Federation of Corrosion Publication No. 18, London, 1996.
[6] P. Castro-Borges, O.T. de Rincon, E.I. Moreno, A.A. Torres-Acosta, M. Martinez-Madrid, A. Knudsen, Performance of a 60-year-old concrete pier with stainless steel reinforcement, Mater. Performance 41 (2002) 50–55.
[7] P. Pedeferri, L. Bertolini, F. Bolzoni, T. Pastore, Behaviour of stainless steels in concrete, in: W.F. Silva Araya, O.T. De Rincon, L.P. O'Neill (Eds.), Repair and Rehabilitation of Reinforced Concrete Structures: The State of the Art, American Society of Civil Engineering, 1998, pp. 192–206.
[8] L. Bertolini, P. Pedeferri, Laboratory and field experience on the use of stainless steel to improve durability of reinforced concrete, Corros. Rev. 20 (2002) 129–152.
[9] FIB, Model Code for Service Life Design, International Federation of Concrete, Bulletin No. 34, 2006.
[10] M.C. Alonso, M. Sanchez, Analysis of the variability of chloride threshold values in the literature, Mater. Corros. 60 (2009) 631–637.
[11] G.K. Glass, N.R. Buenfeld, The presentation of the chloride threshold level for corrosion of steel in concrete, Corros. Sci. 39 (1997) 1001–1013.
[12] L. Bertolini, E. Redaelli, Depassivation of steel reinforcement in case of pitting corrosion: detection techniques for laboratory studies, Mater. Corros. 60 (2009) 608–616.
[13] C.L. Page, Initiation of chloride-induced corrosion of steel in concrete: role of the interfacial zone, Mater. Corros. 60 (2009) 586–592.
[14] U. Angst, B. Elsener, C.K. Larsen, Ø. Vennesland, Critical chloride content in reinforced concrete—a review, Cem. Concr. Res. 39 (2009) 1122–1138.
[15] L. Bertolini, F. Bolzoni, T. Pastore, P. Pedeferri, Behaviour of stainless steel in simulated concrete pore solution, Br. Corros. J. 31 (1996) 218–222.
[16] L. Bertolini, M. Gastaldi, Corrosion resistance of low-nickel duplex stainless steel rebars, Mater. Corros. 62 (2011) 120–129.
[17] A. Poursaee, C.M. Hansson, Potential pitfalls in assessing chloride-induced corrosion of steel in concrete, Cem. Concr. Res. 39 (2009) 391–400.
[18] B.L. Brown, D. Harrop, K.W.J. Treadaway, Corrosion Testing of Steels for Reinforced Concrete, Building Research Establishment, Document 45/78, 1978. (Garston).
[19] G.N. Flint, R.N. Cox, The resistance of stainless steel partly embedded in concrete to corrosion by seawater, Mag. Concr. Res. 40 (1988) 13–27.
[20] K.W.J. Treadaway, R.N. Cox, B.L. Brown, Durability of corrosion resisting steels in concrete, Proc. Instn of Civil Engineers, Part 1, vol. 86, 1989, pp. 305–331.
[21] R.N. Cox, J.W. Oldfield, The long term performance of austenitic stainless steel in chloride-contaminated concrete, in: C.L. Page, P.B. Bamforth, J.W. Figg (Eds.), Corrosion of Reinforcement in Concrete Construction, Society of Chemical Industry, 1996, pp. 662–669.
[22] B. Sorensen, P.B. Jensen, E. Maahn, The corrosion properties of stainless steel reinforcement, in: C.L. Page, K.W.J. Treadaway, P.B. Bamforth (Eds.), Corrosion of Reinforcement in Concrete, Elsevier Applied Science, 1990, pp. 601–610.
[23] U. Nurnberger, W. Beul, G. Onuseit, Corrosion behaviour of welded stainless reinforcing steel in concrete, Otto Graf Journal 4 (1993) 225–259.
[24] U. Nurnberger, W. Beul, Corrosion of stainless steel reinforcement in cracked concrete, Otto Graf Journal 10 (1999) 23–37.
[25] S. Rostam, Service life design of concrete structures—a challenge to designers as well as to owners, Asian J. Civil Eng. 6 (2005) 423–445.
[26] The Concrete Society, Guide to the design of concrete structures in the Arabian Peninsula, Report CS 163, 2008.
[27] T. Pastore, P. Pedeferri, L. Bertolini, F. Bolzoni, A. Cigada, Electrochemical study on the use of duplex stainless steel in concrete, Proc. of Int. Conf. Duplex Stainless Steel'91, vol. 2, 1991, pp. 905–913, (Beaune).
[28] G.G. Clemena, Y.P. Virmani, Comparing chloride resistances of reinforcing bars, Concr. Int. 26 (2004) 39–49.
[29] W.H. Hartt, R.G. Powers, R.J. Kessler, Performance of Corrosion Resistant Reinforcements in Concrete and Application of Results to Service Life Projection, Corrosion 2009, NACE, Houston, 2009, pp. 1–26, (Paper No. 09206).
[30] B. Sederholm, J. Almqvist, S. Randstrom, Corrosion Properties of Stainless Steels as reinforcement in Concrete in Swedish Outdoor Environment, Corrosion 2009, NACE, Houston, 2009, pp. 1–11, (Paper No. 09203).
[31] L. Bertolini, M. Gastaldi, T. Pastore, M.P. Pedeferri, Corrosion behaviour of stainless steels in chloride contaminated and carbonated concrete, restoration of buildings and monuments: an international journal, Internationale Zeitschrift für Bauinstandsetzen und Baudenkmalpfledge 6 (2000) 273–292.
[32] L. Bertolini, M. Gastaldi, P. Pedeferri, E. Redaelli, Factors influencing the corrosion resistance of austenitic and duplex stainless steel bars in chloride bearing concrete, Proc. of 15th International Corrosion Congress—ICC, Granada, September 22–27, 2002, pp. 1–8.
[33] C. Bourgin, E. Chauveau, B. Demelin, Stainless steel rebar: the choice of service life, Proc. of 5th European Stainless Steel Science and Market Congress, Sevilla, September 27–30, 2005, pp. 1–7.
[34] C. Andrade, J.A. Gonzalez, Quantitative measurements of corrosion rate of reinforcing steels embedded in concrete using polarization resistance measurements, Mater. Corros. 29 (1978) 515–519.
[35] P. Ernst, R.C. Newman, Pit growth studies in stainless steel foils. I. Introduction and pit growth kinetics, Corros. Sci. 44 (2002) 927–941.
[36] H. Baba, T. Kodama, Y. Katada, Role of nitrogen on the corrosion behavior of austenitic stainless steels, Corros. Sci. 44 (2002) 2393–2407.
[37] N.J. Laycock, R.C. Newman, Localised dissolution kinetics, salt films and pitting potentials, Corros. Sci. 39 (1997) 1771–1790.
[38] A. Pardo, M.C. Merino, A.E. Coy, F. Viejo, R. Arrabal, E. Matykina, Pitting corrosion behaviour of austenitic stainless steels—combining effects of Mn and Mo additions, Corros. Sci. 50 (2008) 1796–1806.
[39] KyungJin Park, HyukSang Kwon, Effects of Mn on the localized corrosion behavior of Fe–18Cr alloys, Electrochim. Acta 55 (2010) 3421–3427.
[40] G. Rondelli, B. Vicentini, A. Cigada, Influence of nitrogen and manganese on localized corrosion behaviour of stainless-steels in chloride environments, Mater. Corros. 46 (1995) 628–632.